The Solar wind interaction with Venusian Plasma Environment - Analysis of Parker Solar Probe Observations(PSP)

Mohit Dubey
210569166
Supervisior - Dr.David Burgess
SCHOOL OF PHYSICAL AND CHEMICAL SCIENCES
QUEEN MARY UNIVERSITY LONDON

August 31, 2022

Contents

DECLARATION OF THE ORIGINAL WORK

I, Mohit Dubey hereby certify that this Dissertation, which is approximately more than 7500 words in length, has been written by me at the School of Physics and Astronomy, Queen Mary University of London, that all material in this dissertation which is not my own work has been properly acknowledged, and that it has not been submitted in any previous application for a higher degree. This Declaration is made on 31st August 2022.

The sections which contain the report on the independent research work component of the project are Sections 7,8,9,10, 14, and 15
APPENDIX A

ACKNOWLEDGEMENT

My supervisor, Dr. David Burgess, has my gratitude for agreeing to oversee me and for his unwavering support during the research time. Dr. David Burgess assisted me in every way possible with his insightful suggestions, opinions and guidance in completing the research work. I also appreciate Queen Mary University of London for the wonderful opportunity.

Mohit Dubey
School of physical and chemical sciences
Queen Mary University of London

1 Abstract

Due to Venus absence of a magnetic field, the way solar wind interacts with its plasma environment is fundamentally different from how it is on Earth. There is an induced magnetic field on Venus. Venus' ionosphere interacts with the solar wind from the sun to create an induced magnetic field. Despite this, a plasma obstacle forms with some of the same boundaries and structures, including a magnetic tail, bow shock, and fore-shock. Pioneer Venus Orbit (PVO), Venus Express (VEX), and other missions investigated the interaction between the solar wind and Venus. The Parker Solar Probe (PSP) was orbited in August of 2018. To establish the position and shape of the BS, we have employed magnetic field measurements collected by PSP in this work. The PSP data is used to examine the magnetic field structures under this study. The outcomes from PVO, VEX, and PSP data have also been contrasted. Currently, PVO and VEX are the main sources of information for how the solar wind interacts with Venus at this time but PSP data analysis will improve our understanding more in near future new sciences.

2 Introduction

Venus like other planets is under flow of continuous charge from the Sun [24]. The unique thing about Venus is that it does not have an intrinsic magnetic field. Venus has a thick atmosphere, but its upper atmosphere experiences solar wind interaction, which induces a magnetic field. Numerous spacecraft, including Venera 4,6,9, and 10, Mariner 5 and 10, PVO, and VEX, have been launched since the 1960s to study the interaction between the solar wind from Venus and the planet. All of these spacecrafts have demonstrated that the interaction of the solar wind with Venus results in a highly organised plasma (PVO Observations) [22]. VEX also complimented and expanded previous results. Present knowledge of solar wind interaction with Venus comes from a new generation space mission called Parker Solar Probe (PSP). PSP was inserted into the Venus orbit in 2020. Currently, PSP have completed 5 Venus Flyby's (source www.nasa.gov). A supersonic plasma flow is the solar wind. The approaching supersonic solar wind is redirected around the earth by the highly electrically conductive ionosphere. This event causes an upstream wave known as Bow Shock to emerge (BS)[11]

The earliest indication of the obstruction is BS and the corresponding upstream waves. A BS study can reveal a lot regarding solar wind interaction with planetary obstacle. [21] The location and shape of BS have been studied with many models in the past such as MHD model [9] and Hybrid model [2]. In this paper, we will find the shape and location of BS using conic section curve model. [11]. First of the four BS crossing has been analysed with the newly arrived data from the mission. On the PSP, many tools including FIELDs, Sweaps, Wisper, and ISOIS have been installed to gather and deliver data for analysis. Although earlier missions have produced a wealth of observations and findings, PSP will enhance our understanding of the Venus plasma environment (VPE) because to its many special capabilities and newly updated instrumentation. We will learn more about Venus as a result of modified instruments, a closer orbital period, and a distinctive orbital route at solar minimum. We will concentrate on PSP updates and findings in light of prior missions. The paper's objective is to comprehend new findings and revise earlier ones.

3 Literature Review

Venus has been under exploration for over 60 years. The twin Soviet 1VA probes made early attempts to investigate Venus (Sputnik-7, Venera-1). On February 4 and February 12, 1961, the missions were launched, however they ultimately failed. The first successful launch happened on August 27,1962. Venera-4 explored the atmosphere of Venus to a depth of 25 km in 1967. The measurements might be compared after Mariner-5 passed Venus the next day. The Venusian intrinsic magnetic field's highest limit was calculated to be $e - 5$ times greater than that of the Earth [17]. Additionally, bow shock and its related phenomena were found [4].The subsequent Mariner-10 mission measured these enduring characteristics [14]. In 1970, Venera-7 became the first spacecraft to touch down on the surface of Venus. The first spacecraft to transmit data from an extraterrestrial planet's surface was Venera-7.

Venera-9 and -10 accomplished a significant milestone in the study of the Venus-solar wind interaction in terms of space physics. They saw the bow shock, induced magnetosphere barrier, and magneto-tail while orbiting the planet Venus through the night-side tail area [17]The observation of ions with low energy (100-200 eV) in the venus magnetosphere boundary that escaped into space via the magneto-tail was particularly important and remarkable. [17].

The 1978-launched Pioneer Venus Orbiter (PVO), which remained in use until 1992. PVO demonstrated that the interaction of the solar wind with Venus results in a highly organised plasma. Venus Express was launched in 2005, ending a 13-year break that followed the time of intense Venus research (VEX). VEX ran out of fuel after more than 8 years of operation and fell into the sky. VEX enhanced our knowledge and expanded on earlier findings. The numerous spacecraft that have explored Venus have greatly aided ground-based observations in the quest to completely understand our nearest planet. In order to better comprehend Venus' interaction with the solar wind, numerous missions, including Solar Orbiter, BepiColombo, and others, have carried sensors to study the planet's plasma environment. Lastly, the addition of the Parker Solar Probe to the Venusian Plasma Environment (VPE) orbit in 2018 marked a significant advancement in the research of solar-wind interactions with Venus.

4 Venusian Plasma Environment (VPE)

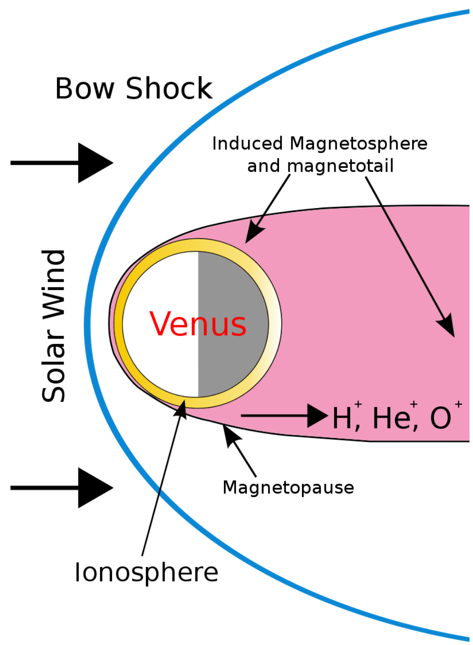

Fig 1. Venus interacts with the solar wind. Components of the induced magnetosphere are shown.

4.1 Upper atmosphere and ionosphere

Height of the Venus' mesosphere ranges from 65 km to 120 km, while the thermosphere starts at a height of around 120 km and finally reaches the exosphere at a height of 220–350 km.When the atmosphere is so thin that there are often fewer than one collisions per air molecule, the exosphere is said to have begun.

Venus has a thick ionosphere that reaches heights of 120–300 km. The thermosphere and ionosphere almost touch. Only the day-side of the planet retains the high levels of ionisation. The concentration of electrons over the night-side is almost nil. Aside from that of Earth, Venus possesses the ionosphere that has been studied and understood the most in our solar system. The Venus ionosphere is not a perfect conductor, thus some magnetic flux can leak into the ionosphere even though it can divert the solar wind to create a bow shock. There are two different states of the ionosphere: magnetised and unmagnetized [3]. The magnetic properties of the ionosphere are significantly influenced by the dynamic pressure of the solar wind, which regulates the height of the ionopause.

4.2 Induced magnetosphere

Everyone is aware that Venus does not have a proper magnetic field like Earth. The cause of its disappearance is unclear, however it might be connected to a weaker convection in the Venusian mantle. Venus only has an induced magnetosphere, which is a product of the solar wind carrying the magnetic field of the Sun. It is possible to visualise this process as the field lines encircling an obstruction—in this case, Venus. Venus's induced magnetosphere is composed of a current sheet, a magneto-sheath, a magneto-pause, and a magneto-tail.

According to earlier studies, the magneto-sheath of Venus is home to several strong magnetic field variations that can be formed locally or convect from the upstream foreshock. [18]. When it comes to the movement of momentum and energy within the planet's space plasma environment, magnetic field fluctuations are crucial [19]. In the lack of high-resolution plasma data, the study of magnetic fluctuations is essential.

Since Venus lacks a magnetic field, it has extremely different atmospheric escape and energy deposition processes than Earth. The solar wind can interact directly with Venus' upper atmosphere despite its magnetic field. A sizable amount of the exosphere is destroyed by plasma flow through the processes of photo ionisation, charge exchange, and electron impact ionisation as a result of the shocked solar wind flow. Between the shocked solar wind flow and the ionosphere, tail-ward convection of the plasma mantle causes another sort of atmospheric loss.

Significant sputtering could be caused by ions that are re-entering the atmosphere as a result of their gyrating along magnetic field lines buried in the plasma. The degradation of the Venusian ionosphere under diverse solar wind conditions is another process for the loss of atmospheric components. The solar wind interacts with the top of the ionosphere on the planet's night side, where the majority of the planet's mass is lost, to produce a complex array of plasma clouds, tail rays, filaments, and ionospheric holes.

4.3 Venusian Bow Shock

Although bow shocks happen around every planet, including magnetised ones like Jupiter and Saturn and unmagnetized ones like Mars and Venus, they happen when the Sun's wind collides with Earth's magnetopause. Even though Venus has no detectable intrinsic magnetic field, the solar wind is nonetheless deflected about the ionopause, creating a disconnected bow shock, because the diffusion period of the magnetised solar wind plasma into the ionosphere is often quite long at solar maximum. By dividing the PVO shock crossings into several categories according to the solar wind plasma properties, it has been possible to deduce the effects of the solar wind dynamic pressure, Mach numbers, IMF orientation, and solar cycle on the bow shock.[23].

4.4 Wake

The magneto-tail of Venus is clearly delineated [12]. The magnetic field lines travelling close to the planet will gather mass from the atmosphere and ionosphere and slow down in order to wrap around the impediments. The magneto-tail is produced by the slowing of magnetic flux tubes that were convected past the planetary obstruction. It was demonstrated by [10] that the induced magnetic field (IMF) around rather than merely diverted around the planetary obstacle.

5 Parker Solar Probe and its instrumentation

The Parker Solar Probe was launched by NASA in 2018 with the intention of conducting research on the Sun's outer corona. It will pass within 9.86 solar radii of the Sun's centre (6.9 million kilometres or 4.3 million miles), and by 2025, it will be moving at a maximum speed of 690,000 kilometres per hour during its closest approach. It is among the quickest spacecraft ever constructed.

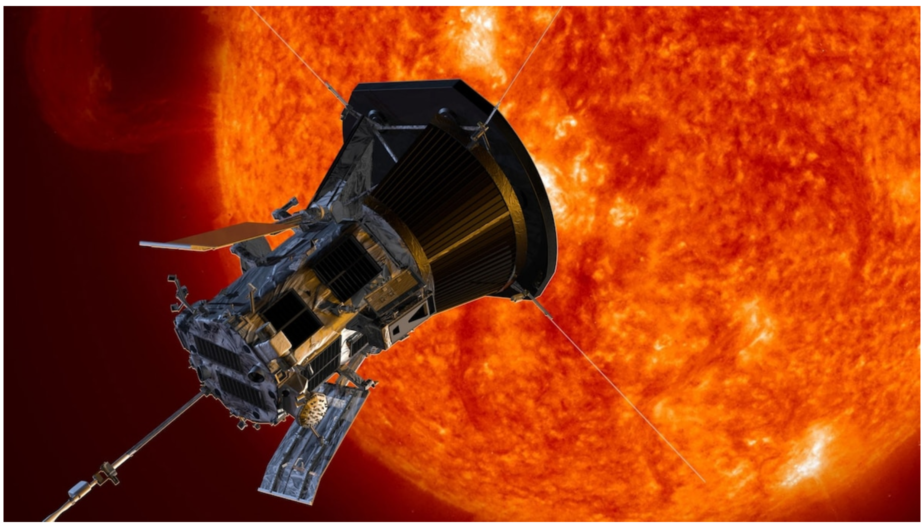

Parker Solar Probe

5.1 FIELDs

PSP have five antennas,Out of five, four of which protrude over the heat shield of the spacecraft, where they reach temperatures of 2,500 degrees Fahrenheit, FIELDS analyses the electric field surrounding the spaceship. An alloy of niobium, which can resist extremely high temperatures, is used to create the 2-meter-long antennas. FIELDS measures electric fields directly, or in situ, as well as remotely, over a wide frequency range. The four sunlit antennas, which operate in two modes, gauge the characteristics of the fast and slow solar wind, which is the continuous flow of solar particles emanating from the Sun. In order to provide a three-dimensional image of the electric field at higher frequencies, the fifth antenna, which protrudes perpendicular to the others in the shade of the heat shield, is used.

Measurement of the the large-scale coronal magnetic field is done by the identical fluxgate magnetometers MAGi and MAGo Since it can sample the magnetic field at a rate of two million times per second, the search coil magnetometer is necessary closer to the Sun where the magnetic field is subject to rapid change. For measuring the magnetic field farther from the Sun, where it varies more slowly, fluxgate magnetometers are designed.

5.2 IS0IS

The Integrated Science Research of the Sun (IS0IS), uses two complementary equipment in a single, integrated scientific research to track particles at various energies. The abbreviation contains the Sun's sign. IS0IS will be able to comprehend the life cycles of the particles, including where they came from, how they were accelerated, and how they departed the Sun through interplanetary space, by observing electrons, protons, and ions. EPI-Lo and EPI-Hi are the names of the two energetic particle experiments aboard ISIS (EPI stands for Energetic Particle Instrument).

Carbon, oxygen, neon, magnesium, silicon, iron, and the two isotopes of helium, He-3 and He-4, are all identified by EPI-Lo by measuring the spectra of electrons and ions. It will be possible to identify which of numerous proposed mechanisms caused the acceleration of the particles by distinguishing between helium isotopes. A large field of view is offered by numerous viewfinders for the observation of low-energy particles. A carbon-polyimide-aluminum ion enters EPI-Lo through one of the viewfinders, travels through two of these foils, and finally comes into contact with a solid-state detector. The foils produce electrons when they collide, and a micro-channel plate measures these electrons.

To monitor particles with energy greater than those observed by EPI-Lo, EPI-Hi makes use of three particle sensors made of stacked layers of detectors. Geometric segmented ultra-thin silicon detectors are used in the first few layers to assist decrease background noise and determine the direction of the particles. Ionization, the process by which charged particles remove electrons from atoms in individual detectors, is used to measure the depth to which charged particles penetrate the stack of detectors and to identify charged particles.

5.3 SWEAP

Solar Probe Cup (SPC) and the Solar Probe Analyzers (SPAN) are two complementing devices used in the Solar Wind Electrons Alphas and Protons research, or SWEAP, for the observations. The instruments monitor characteristics including density, velocity, and temperature as well as count the most abundant particles in the solar wind, including protons, electrons and helium ions.

While SPAN-B solely examines electrons, SPAN-A consist of two components to measure both electrons and ions.

5.4 WISPR

The only imaging instrument on board the spacecraft is the Wide-Field Imager for Parker Solar Probe. Before the spacecraft passes through the corona and solar wind, WISPR examines their large-scale structure. The cardboard box WISPR instrument observes solar ejects such as coronal mass ejections or CMEs, jets, and other structures from a distance. The spacecraft's other instruments conduct in-situ observations as these formations move away from the Sun and finally pass over it. WISPR aids in connecting the intricate physical measurements being taken immediately in the vicinity of the Sun to what is occurring in the large-scale coronal structure.

Specially designed baffles and occulters scatter and absorb any residual stray light that has been diffracted or reflected off the edge of the heat shield or other sections of the spacecraft. Two radiation-resistant Active Pixel Sensor CMOS cameras are used by WISPR. Due to their reduced weight and lower power consumption, these detectors are employed instead of conventional CCDs. Additionally, they are less vulnerable to the harmful effects of cosmic rays and other high-energy particles, which are a major worry in the vicinity of the Sun. The camera's lenses are constructed from radiation-hard BK7 glass, which is more often used for space telescopes and is sufficiently hardened to sustain impacts from dust.

6 Venus Coordinate System

The Venus Solar Orbital (VSO) coordinate system is being used to archive the Galileo trajectory data. The Geocentric Solar Ecliptic (GSE) coordinate system, as suitably described for Venus, is essentially the basis of the VSO coordinate system. Along the Venus-Sun line, the VSO X is pointed positively toward the Sun. The VSO's Z and Y directions are positive northward and parallel to the Venus orbital plane's normal, respectively. Z completes the right-handed set (towards dusk).

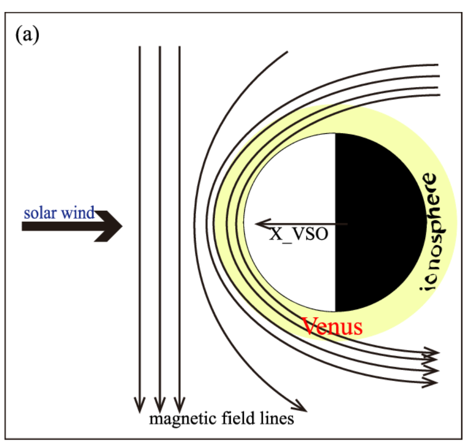

Fig. 2 VSO Coordinate System

7 Parker Bow Shock Crossing

The Parker solar probe has performed five flyby's till October 2021. PSP is scheduled for Seven Venus Flyby's. The final Venus Flyby will take its closest approach of Venus in November 2024.(source: www.sppgway.jhuapl.edu) Here, we will study the first four Flyby of PSP:

7.1 Venus Flyby 1

PSP crosses bow shock for the first time on 3rd October 2018 at 8:44 UT. A fast magneto sonic shock wave was observed. [22] The orbit was highly elliptical around the Venus and the perihelion was 2548km. FIELDS receives fluctuations from 8:01AM till 8:45AM UTC. The closest encounter with Venus occurs at 8:44AM UTC (Fig 1.b). Thereafter, PSP changes its trajectory and the fluctuations stopped occurring. Fig. 3 clearly shows the trajectory change in PSP. The fig.3.b trajectory for the shock is taken for a period of 1hr.

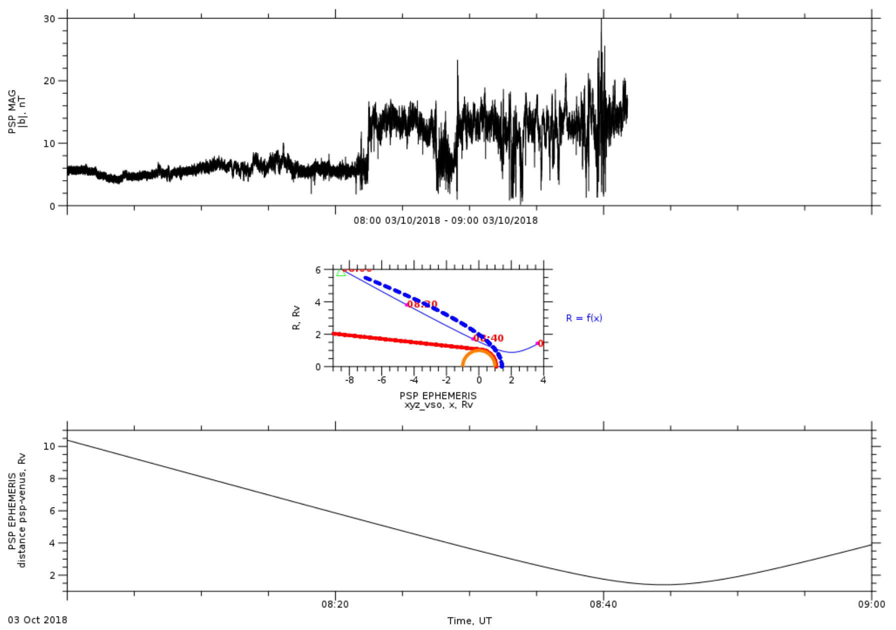

Fig.3.a FIELDS total magnetic field strength (PSP MAG), 3.b PSP ephemeris(Distance vs time) inside BS, 1.c Trajectory changes according to time

When PSP enters the magnetic field of Venus, the magnetometer MAG measures magnetic field vector. Magnetometer Fluxgate, Parker Solar Probe FIELDS Instrument Suite, MAG, Data: The MAG time series data's temporal resolution changes depending on the instrument mode and ranges from 2.289 samples/s to 292.9 samples/s. These two data sampling rates correspond to two samples per 0.874 seconds or 256 samples per 0.874 seconds, where 0.874 s = 225 divided by 38.4 MHz. The four ranges of the magnetometer are 1024 nT, 4096 nT, 16,384 nT, and 65,536 nT. Based on the strength of the surrounding magnetic field, an algorithm chooses the magnetometer range. According to the 16-bit Analog to Digital Converter, the magnetic field measuring precision is range about 15 bits. The PSP MAG measures three highest peaks in total magnetic field strength $|b|$of reading 16nT, 24nT, 30nT. All other readings measures in the range of 10-20nT. From the fig.4 it can be clearly identify that the spacecrafts travels through the edge of the Venusian BS. Throughout travel PSP never enters into the ionosphere of Venus.

The data stopped coming after 8:42AM UT. PSP MAG also stopped showing fluctuation. During the closest approach a technical glitch was observed in the system and due to this glitch it was not able to collect the data. Fig 4 shows the plotting of coordinates bx nT,by nT,bz nT. In the coordinates sharp boundaries are observed. The structure formed in the coordinates is quasi-perpendicular.

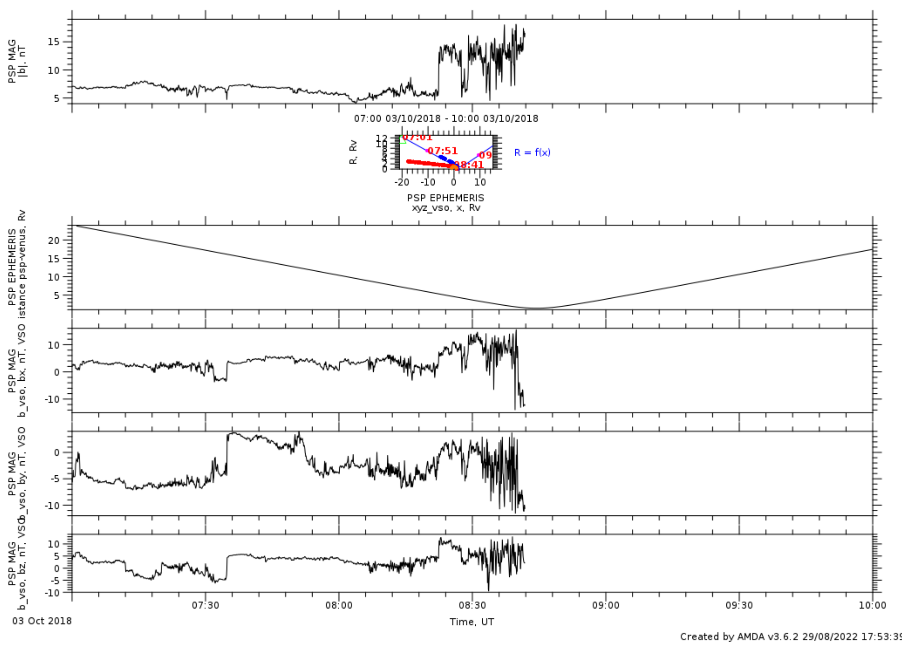

Fig.4.a FIELDS total magnetic field (PSP MAG), 1.b PSP ephemeris(Distance vs time) inside BS, 4.c,d,e coordinates total magnectic field strength bx nT, by nT, bz nT

7.2 Venus Flyby 2

PSP for 2nd Flyby passes the bow shock on 26 December, 2018, at 18:14 UTC. Supersonic solar wind caused a swift magneto sonic shock wave, which was seen. The perihelion distance was 3023 kilometres, and the orbit around Venus was very eccentric. Variations are received by FIELDS from 17:50 to 18:20 UTC. At 18:14 PM UTC, Venus and the Earth make their closest approach. The variations then stop after PSP modifies its trajectory. The trajectory change in PSP is clearly depicted in (Fig.5.b) but there is a also small variation in MAG when PSP changed the direction. This variation is visible at 18.20 UTC. The variation was observed far from the bow shock. The fig.5.b trajectory for the shock is taken for a period of 1hr.

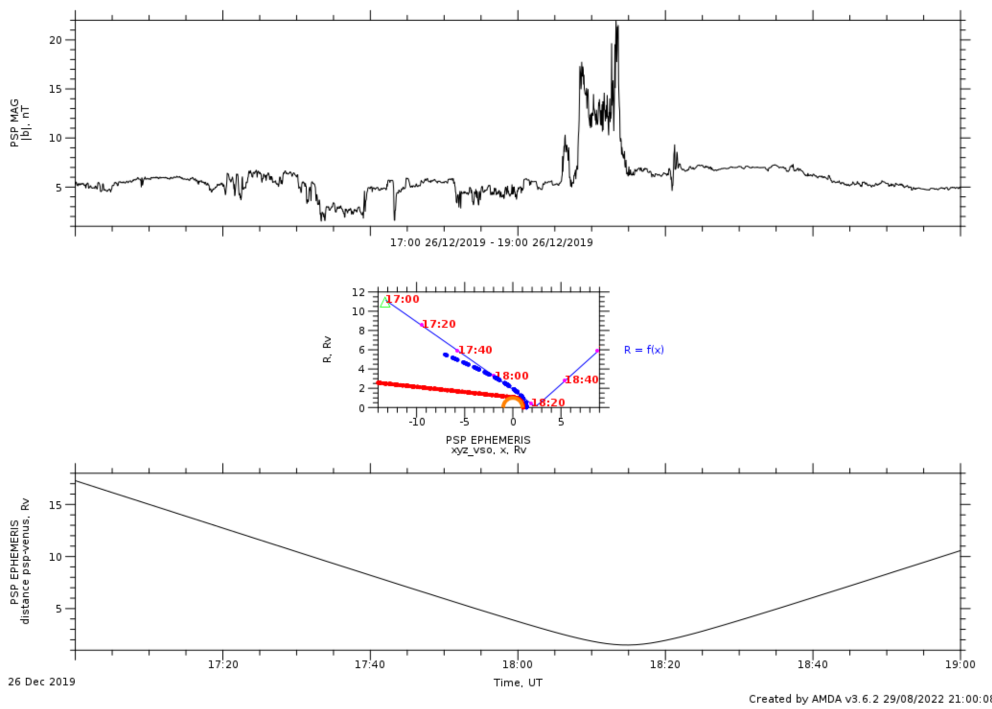

Fig.5.a FIELDS total magnetic field strength (PSP MAG), 5.b PSP ephemeris(Distance vs time) inside BS, 5.c Trajectory change according to time

The special thing about this encounter is that PSP slides through the boundary of BS. In the trajectory its clearly visible that PSP was travelling on the edge of BS. Again, when PSP enters the magnetic field of Venus, the magnetometer MAG measures total magnetic field strength. The two highest peaks in the total magnetic field strength $|b|$, measured by the PSP MAG, are 18nT, 22nT. All other measurements fall between 10 and 16 nT. It is evident from Fig. 5 that the spacecraft passes through the edge of the Venusian BS. PSP never enters the Venus ionosphere when travelling. At 18:20 UTC, an unusual magnetic field fluctuation with a strength of 8 nT occurred (Fig 5 a). After 18:20 UTC, the data stopped coming. The PSP MAG ceased displaying fluctuation as well. Figure 6 has the coordinates bx nT, by nT, and bz nT plotted. Sharp boundaries are seen in the coordinates. In the coordinates, a quasi-parallel structure has been produced.At the same location in Venus's orbit, flybys 1 and 2 take place.

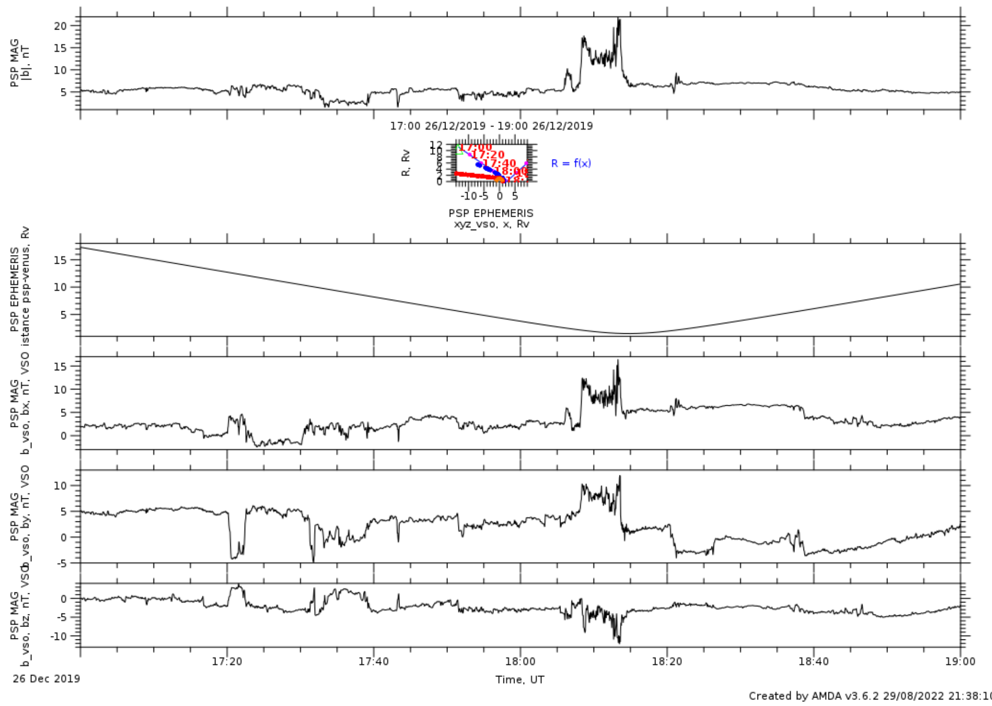

Fig.6.a FIELDS measures total magnetic field (PSP MAG), 6.b PSP ephemeris(Distance vs time) around BS, 6.c,d,e coordinates total magnetic field strength bx nT, by nT, bz nT

7.3 Venus Flyby 3

On July 11, 2020, at 3:22 UTC, PSP passed for the 3rd time around Venus Bow shock. Many quick magneto sonic shock wave was produced by the supersonic solar wind and was observed. The orbit around Venus was extremely eccentric, and the perihelion distance was 824 kilometres. FIELDS received various variations between 03:15 and 04:20 UTC. PSP make their closest approach at 03:22 UTC (Fig 7.b). Inside the bow shock, the many spectacular variation was seen. The shock's track in Fig. 7.b is recorded for a duration of one hour. PSP enters the Venusian Ionosphere for the first time. Firstly, it crosses the BS and then escaped into the ionosphere and changes its direction very rapidly. It was in ionosphere for 10-20 minutes(approximately). Between Ionosphere PSP and BS spent approximately 5-15 minutes.(Fig. 7 b)

When PSP entered the BS a quick magneto sonic shock wave was produced by the supersonic solar wind (Fig 8 a) at 3:22 UTC. Thereafter, when it approaches the ionosphere, circular and blunt shaped movement waves in the MAG was observed. Many dips in the waves were observed. The two highest peaks in the total magnetic field strength $|b|$, measured by the PSP MAG, are 12nT,

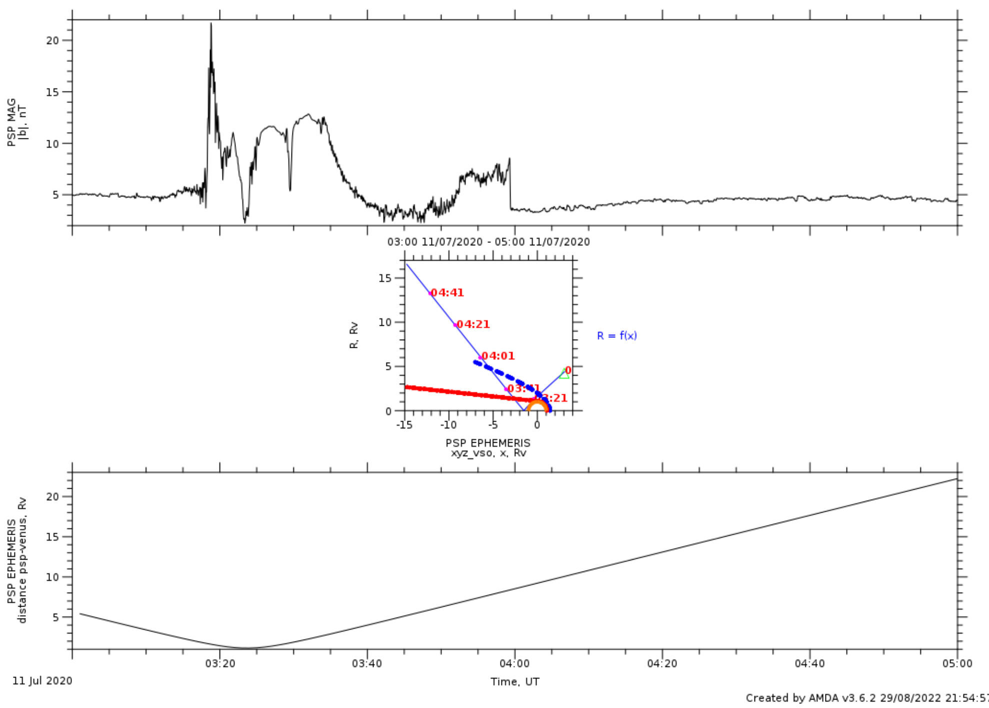

Fig.7.a FIELDS total magnetic field strength (PSP MAG), 7.b PSP ephemeris(Distance vs time) inside BS, 7.c Trajectory changes according to time

22nT. All other measurements fall between 01 and 10 nT. It is evident from Fig. 8 that the spacecraft passes through the ionosphere of the Venus. After 3:55 AM UTC, the data stopped coming. Figure 8 has the coordinates bx nT, by nT, and bz nT plotted. Sharp and blunt circular boundaries are seen in the coordinates. In the coordinates, a quasi-perpendicular structure can be seen.

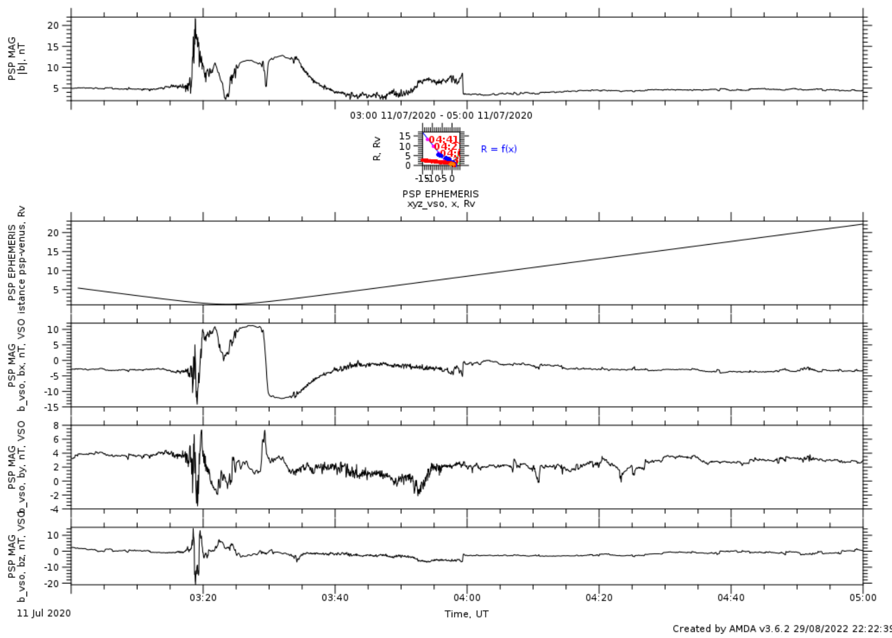

Fig.8.a FIELDS measures total magnetic field (PSP MAG), 8.b PSP ephemeris(Distance vs time) inside BS, 8.c,d,e coordinates total magnetic field strength bx nT, by nT, bz nT

7.4 Venus Flyby 4

PSP passed around the Venus Bow shock for the fourth time at 19:55 UTC on February 20, 2021. The supersonic solar wind generated and recorded numerous fast magneto sonic shock waves. The perihelion distance was 2392 kilometres, and Venus' orbit was very eccentric. Between 19:55 and 20:30 UTC, FIELDS MAG got several variations. At 19:55 UTC, PSP makes their closest approach (Fig 9.b). There were numerous stunning variations visible inside the bow shock and magnetic field. The shock track in Fig. 9.b is captured over an two hour-long period of time. PSP makes its second ascent into the Venusian ionosphere. Again, it first crosses the BS, then eludes into the ionosphere and abruptly alters course. It spent 20 minutes in the ionosphere (approximately). Among the Ionosphere PSP passed around the Venus Bow shock for the fourth time at 19:55 UTC. Between Ionosphere and BS, PSP spent approximately 30 minutes approx).(Fig 9 b)

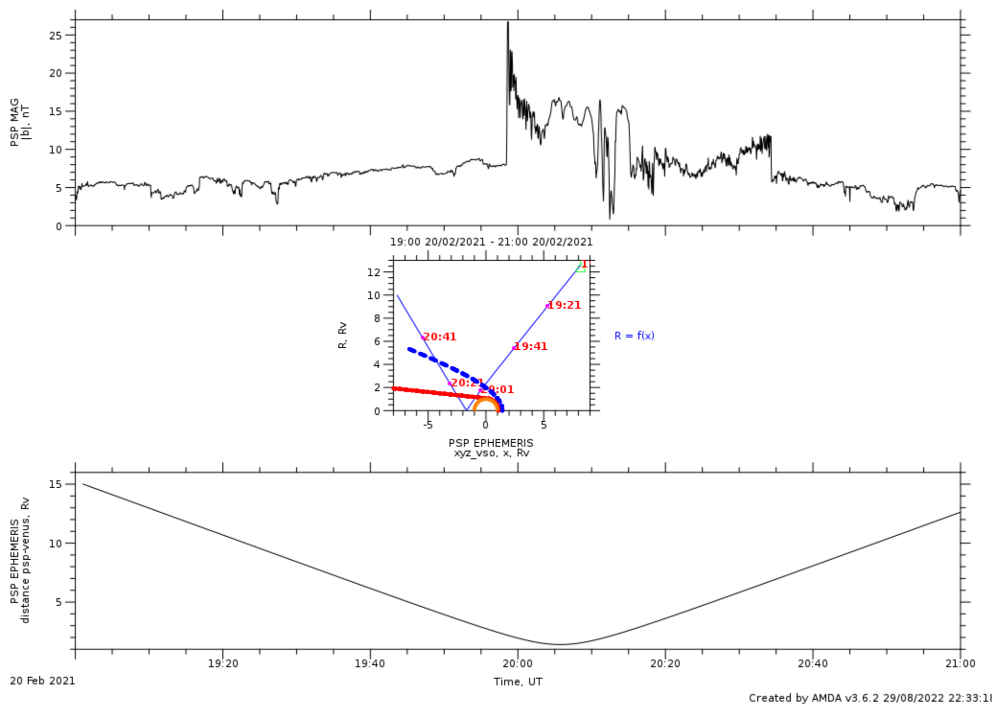

Fig.9.a FIELDS total magnetic field strength (PSP MAG), 9.b PSP ephemeris(Distance vs time) inside BS, 9.c Trajectory changes according to time

When PSP entered the BS a quick magneto sonic shock wave was produced by the supersonic solar wind (Fig 3 a) at 3:22 UTC. Thereafter, when it approaches the ionosphere, many blunt shaped movement waves in the MAG was observed. Many dips in the waves were observed. The one highest peaks in the total magnetic field strength $|b|$, measured by the PSP MAG, are 28nT. All other measurements fall between 01 and 15 nT. It is evident from Fig. 9 that the spacecraft passes through the ionosphere of the Venus. After 20:40 UTC, the data stopped coming. Figure 4 has the coordinates bx nT, by nT, and bz nT plotted. Blunt peaks are seen in the coordinates. In the coordinates, a quasi-perpendicular structure can be seen.

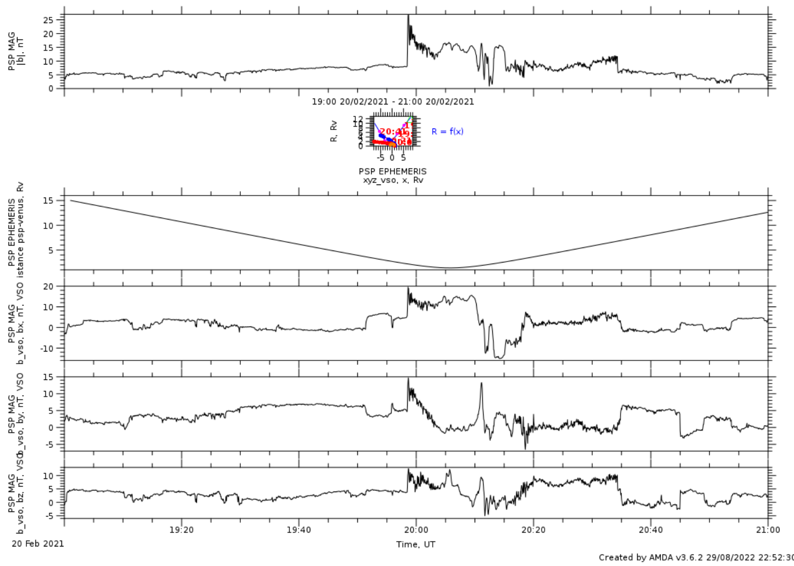

Fig.9.a FIELDS measures total magnetic field (PSP MAG), 9.b PSP ephemeris(Distance vs time) inside BS, 9.c,d,e coordinates total magnetic field strength bx nT, by nT, bz nT

8 Venus Flyby Plotting around BS

Due to a paucity of data and a spacecraft malfunction during the encounter, plotting of Venus Flyby 1 has not been done.

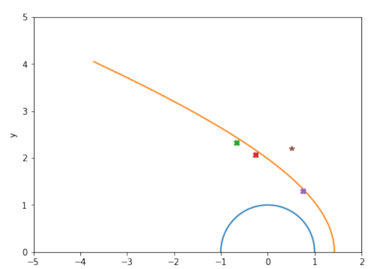

Venus Flyby 2 (The character (*) denotes the PSP crossing around BS)

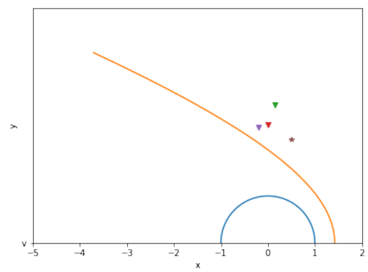

Venus Flyby 3 (The character (v) denotes the PSP crossing around BS)

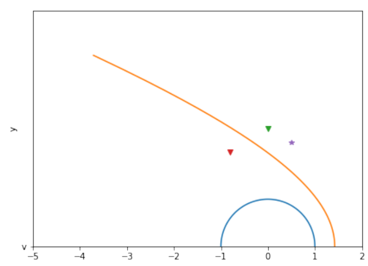

Venus Flyby 4 (The character (v) denotes the PSP crossing around BS)

9 Location and shape of the Bow shock

From 2018-10-03 to 2021-02-20, four Venusian BS flyby's were identified from the PSP reconstructed data. On some close encounters PSP made some serious entrance into the Venusian BS as well the ionosphere. Because a technical issue was noticed during the closest contact, it was challenging to analyse the flyby 1 data. We excluded these cases from our analysis and the final results in order to avoid outliers.

The Sun's intense ultraviolet (EUV) light causes the bow shock to move. The exosphere and upper atmosphere warm as a result of increased EUV radiation, which also increases the scale height. Ion generation is enhanced due to the correspondingly increased photo-ionization rates and greater scale height. The wind solar plasma then receives a bigger mass charge from these higher atmospheric ions, which forces the arc shock outward. As a result, a number of factors, such as the Mach number of the solar wind and the wave's relative speed to the solar wind, affect the location of BS.

A change in the magnetic field's amplitude relative to the upstream region that indicates the presence of a bow shock is also used to locate them and compare them to prior and subsequent orbits. While we choose the centre of the transition period between the upstream solar wind and magneto-sheath for the quasi-parallel bow shock, we choose the medium of the ramp for the quasi-perpendicular bow shock. The shock location has no error bars. Up to 2020, PSP completed four successful flybys of the Venusian Bow Shock. The following list includes the various shock positions for 3 flybys:-

9.1 Venus Flyby 2 (Table 1)

Time	Position(x,y,z) R_v	Shock normal(nx,ny,nz)
18:06:20	-0.661,-2.327,-0.118	(0.486,-0.873,-0.042)
18:08:30	-0.259,-2.066,-0.118	(0.521,-0.852.-0.046)
18:13:37	0.745,-1.303,-0.118	(0.687,-0.724,-0.064)

9.2 Venus Flyby 3 (Table 2)

Time	Position(x,y,z) R_v	Shock normal(nx,ny,nz)
03:18:20	(0.15, -2.2,-1.95)	(0.573, -0.630, -0.524)
03:18:40	(0, -1.6, -1.95)	(0.566, -0.548, -0.616)
03:19:25	(-0.2, -1.5, -1.95)	(0.548, -0.538, -0.640

9.3 Venus Flyby 4 (Table 3)

Time	Position(x,y,z) R_v	Shock normal(nx,ny,nz)
19:58:50	(0, -2.5, 2.7e$^(-3)$)	(0.551, -0.835, 0.000)
20:01:58	(-0.8, -2, 2.85e$^(-3)$	(0.461, -0.887, 0.00)

Table 1 contains the time, location, and shock normal values. Each section's three intervals were taken and plotted in the Python code as well. Angles of 82, 84, and 101 degrees exist between location and shock normal for encounter 2.

Table 2 contains the values for time, position, and shock normal. Three intervals of each value have been chosen, and the python code has also been used to plot them. For encounter 3, the angles between position and shock normal are 81.5, 83, and 88 degrees.

Table 3 contains the values for time, position, and shock normal. Three intervals of each value have been taken, and the python code has also been used to plot them. For encounter 4, the angles between position and shock normal are 79 and 84 degrees.

In order to account for Venus's orbital speed (35 km/s), we first determined the shock positions into VSO coordinates. Then, we transormed the data into an aberrated solar ecliptic system, along with the assumed angle of 5 degrees from VSO. A conic section curve is then fitted to the shock's shape, and the equation for the conic section is R = L/ 1+ ϵ cos θ where R is the observed bow shock distance from the conic focus, and the polar coordinates (r, θ) are measured with respect to a focus located at (x0; 0; 0), L is the conic section semi-latus rectum, is the eccentricity.

This method is frequently used to determine the shape of the BS. Some studies use the planet's centre as the focus when using this popular method, called the conic section curve [20], while others let the focal point along the Sun-Venus be a free parameter [11]. Additionally, a parabola provides a suitable match [6]. The models are stitched together with an asymptotic shock cone (Mach cone) on the night-side and are valid for solar zenith angles up to 90–120°[20]

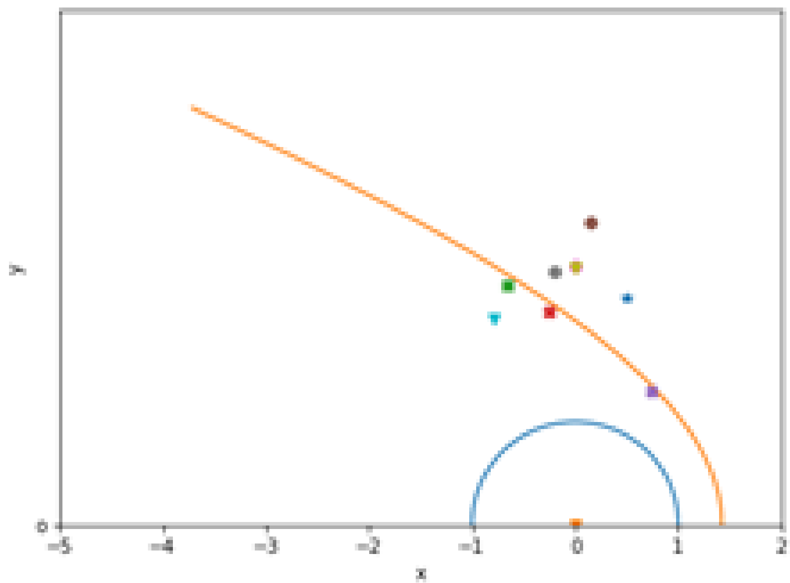

Fig. 11 – Displays the BS fits of all three Venus Flyby's using the ephemeris and FIELDS observations in an aberrated VSO coordinated system. The orange curve is the fit to all BS crossings. Using a conic section curve with a fixed focus and eccentricity and a variable L, all BS crossings were extrapolated to the terminator plane . (*) denotes flyby 2 and (v) denotes flyby 3,4.

Numerous studies present slightly different findings depending on the spacecraft (Venera-9/10, PVO, VEX, or PSP), the kind of data analysed, the time frame used, and the fitting technique. The subsolar bow shock is always well above the obstruction, regardless of the model, and is thus entirely detached even during the solar minimum. We observed that the data on the day-side and the night-side cannot be represented by a single conic function, as was also highlighted in the case of the magnetic pile-up boundary (MPB) at Mars, thus we utilised a somewhat different methodology to simulate the position of the ICB [8]. As a result, the measurements were split into observations from the dayside (X> 0) and the nightside (X<0). On the dayside, the ICB crossings were fitted with a circle (r c = 1.10), whereas on the nightside, the data set was fitted with linear regression.

9.4 Shape of the shock

The magnitude and shape of the bow shock are mostly determined by the size of the obstruction, but the PVO and VEX studies demonstrate that solar cycles also play a role. Even though Venus has no detectable intrinsic magnetic field, the solar wind is nonetheless deflected about the ionopause, creating a disconnected bow shock, because the diffusion period of the magnetised solar wind plasma into the ionosphere is often quite long at solar maximum. At solar minimum, middle, and maximum circumstances, it changes. Results from PVO and VEX show that solar activity can affect how the Venusian bow shock behaves since the bow shock terminator distance was found to be greater at solar maximum than at solar minimum. [15]. The range of the solar zenith angle (SZA)at the Venusian bow shock covered by PVO is limited from 60 degree to 110 degree [15] , and the subsolar location cannot be well defined. The VEX mission covers a range of SZA (10 to 135 degree) at the Venusian bow shock, and both the standoff and terminator distance of the Venusian bow shock can be accurately calculated [24] . In PSP data, where the shock is farther away from Venus at solar maximum and intermediate is confirmed. Shock also changes the size according to the solar wind conditions.

In PVO and VEX results, at intermediate solar activity, the subsolar bow shock is at an altitude of 2200-2300 km(approx.). At solar minimum the subsolar shock altitude decreased to 1700-1800 km(approx.), a large decrease but still well above the Venus' ionopause. In PSP observations, the fluctuations observed in shock around 850 km altitude in the insert of Venus Fly by 3 at solar minimum. Results show that even if the shock is detached, the effective altitude of the obstacle, calculated from the [16], is close to 0 km, indicating that the obstacle is weak and that significant solar wind absorption is occurring. The shock is separated, as shown by the outcomes. At solar minimum there are no in situ PSP measurements of the ionopause due to less number of shock crossing. In order to get a more clarity ICB fit from PSP data it is necessary to include remaining crossing of PSP around Venus BS and ionosphere. In the meantime more closer PSP flyby's will able to give better results. To study the ionopause as determined by [11]

Unfortunately, due to lack of crossings and data sets, it becomes too difficult to calculate the values of terminator at different solar wind phases. But with the observation and data it is obvious that the BS position and shape around the Venus is also dependent on the phases of solar cycles. Previously it is investigated with the data that at solar minimum condition the BS found to be closer to the planet than at solar maximum by other PVO, VEX and other space missions because of the lower ionization, ion pickup rates. From (Fig 11) the plotted data set we do not observe yet an effect on terminator BS position and shape because EUV flux variation is small over the orbit of PSP. However, it can be concluded from the measurements and observations BS position is stable and in the night-side the ICB is highly variable.

9.5 Effect of Alfven Mach Number

Solar wind activity can have a significant impact in extremely dire circumstances. BS crossings were seen by PVO, VEX, and PSP while they were incredibly far from the earth. All the anomalous shock location are all attributed towards low Mach number. Previously discussed model showed that at low Mach numbers the shock locations are very sensitive to changes of the Mach Number [5]. This sensitivity to the Mach number also involves sensitivity to the direction of the interplanetary magnetic field, as the magneto sonic velocity depends on the angle between the ambient magnetic field and the propagation direction. As a result, the Mach number is influenced by the angle between the magnetic field and the shock normal. In PSP BS crossing on all Venus Flyby 2, 3 and 4 we see many times the sudden high rise in the magnetic field which signifies that average magnetic field was higher than normal leading to a dropping of the Alfvén Mach number and also of magneto sonic Mach number. We have seen a low mach number, but with more in-depth examination in the future, all values and angles can be looked at to get more useful data. Then, the newly obtained values and the earlier outcomes can be compared.

10 Changes in Magnetic field Lines during 4 Venus Flyby's

10.1 Venus Flyby 1

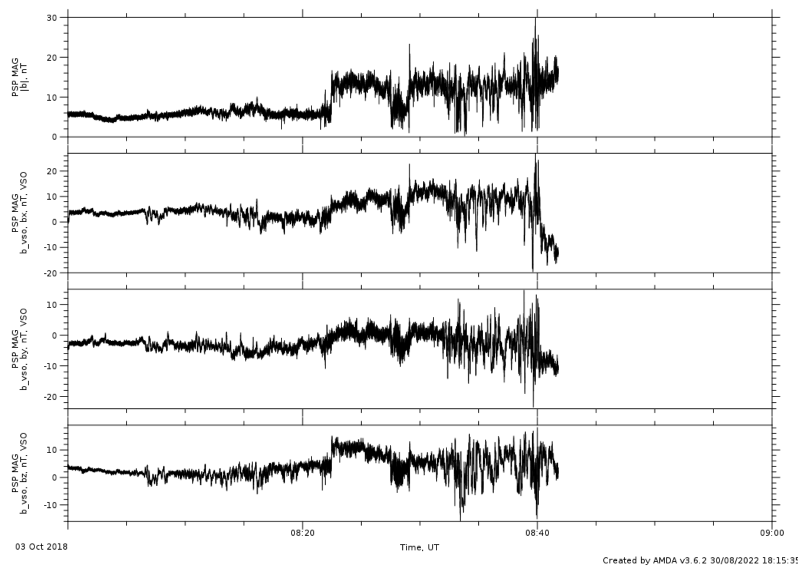

Fig. 12.a.total magnetic field $|b|$ nT, 12.b,c,d VSO coordinates bx nT, by nT, bz nT

When PSP entered the BS, there were visible, extremely abrupt and quick changes in the magnetic field. FIELDs recorded variations between 8:22 and 8:44 UTC.The crossing's geometry was quasi-perpendicular. 20 nT is the typical magnetic field strength.

10.2 Venus Flyby 2

The magnetic field changed visibly, abruptly, and quickly when PSP reached the BS during second encounter. Sudden massive changes over frequent time intervals are visible in the magnetic field. Variations between 18:05 and 18:25 UTC were captured by FIELDs.Overall for 20 minutes the fluctuations appeared. The geometry of the crossing was quasi-perpendicular since the position and shock normal were at an angle of QBn = 81°,84°,101°(Q is theta). The usual magnetic field intensity is in range 16-20 nT.

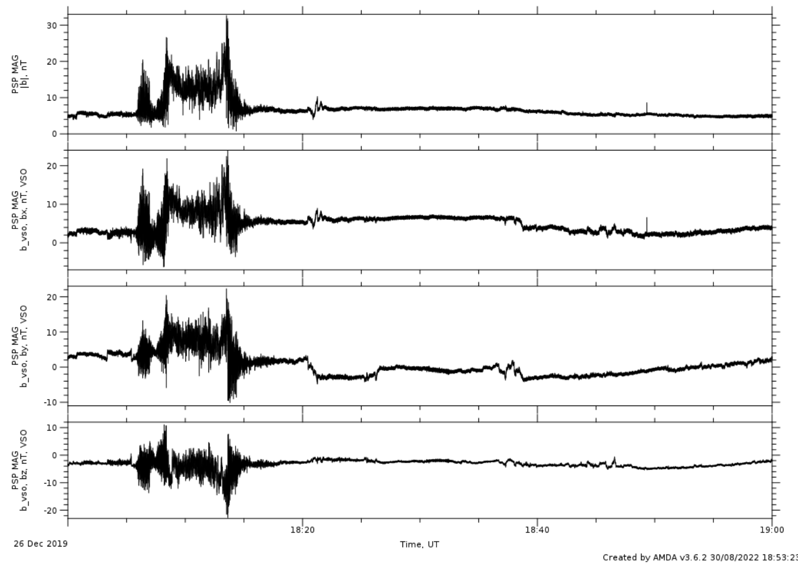

Fig. 13.a.total magnetic field $|b|$ nT, 13.b,c,d VSO coordinates bx nT, by nT, bz nT

10.3 Venus Flyby 3

When PSP arrived at the BS on the third encounter, the magnetic field shifted visibly, unexpectedly, and quickly. The magnetic field can be seen to undergo abrupt, significant shifts over a number of time intervals. Shifts were dipping and the variations sometimes were sharp as like other two previous encounters but sometimes it was not. There is a massive dip FIELDs recorded variations between 03:19AM UTC and 04:00AM UTC. Overall, the fluctuations were visible for 40 minutes. Given that the position and shock normal were at an angle of QBn = 81°, 84°, and 101°(Q is theta), the geometry of the crossing was quasi perpendicular in the beginning but it changed to quasi parallel after few minutes. Over the course of time it changes abruptly as PSP travels ahead in the orbit .The typical range for magnetic field strength is 12 nT.

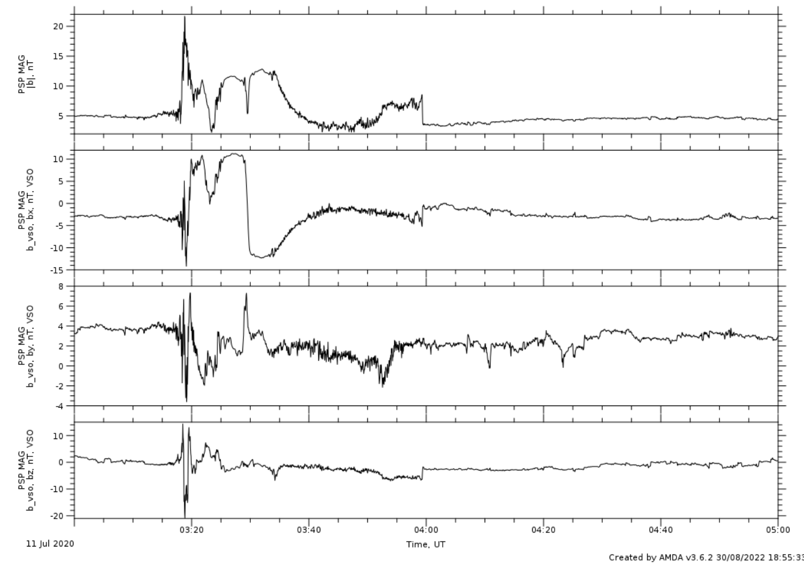

Fig. 14.a.total magnetic field $|b|$ nT, 14.b,c,d VSO coordinates bx nT, by nT, bz nT

10.4 Venus Flyby 4

On the fourth encounter, the magnetic field noticeably, abruptly, and rapidly changed when PSP reached the BS. Over a range of time scales, it is possible to observe the magnetic field undergoing abrupt, large alterations. Variations were captured by FIELDs between 20:00 and 21:25 UTC. The variations could be seen for a total of the approximately one hour. The geometry of the crossing was quasi perpendicular initially and also sometimes it was quasi parallel because the location and shock normal were at angles of QBn = 81°, 84°, and 101°(Q is theta). The magnetic field strength typically falls between 5 and 15 nT.

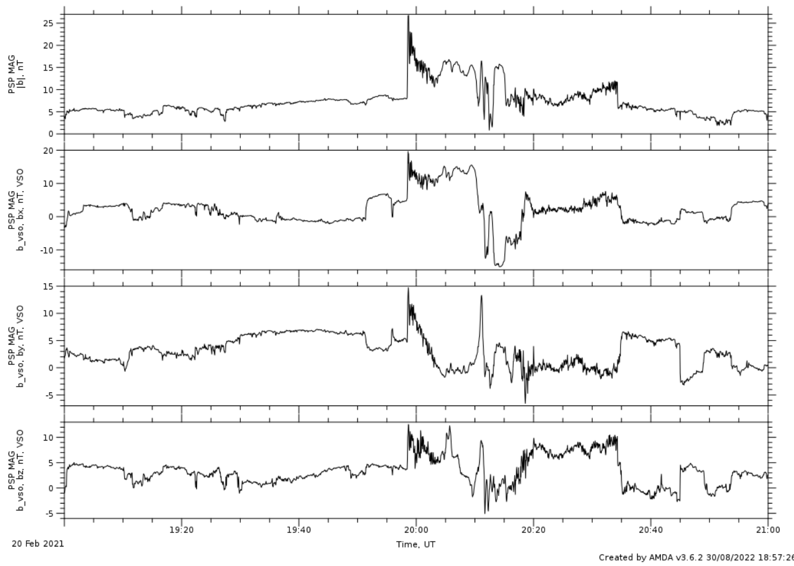

Fig. 15.a.total magnetic field $|b|$ nT, 15.b,c,d VSO coordinates bx nT, by nT, bz nT

Fig. 15.a.total magnetic field $|b|$ nT, 15.b,c,d VSO coordinates bx nT, by nT, bz nT

11 Polarisation of Magnetic Field

The polarisation characteristics of plane waves can be analysed using one of three methods [1] . All techniques imply that a single dominating major plane wave mode propagates perpendicular to the plane. The parameters identified by the analysis are the average of the characteristics for each individual wave when there are many waves at the same frequency. The three methodologies' methods for determining the transformation to the primary plane fundamentally differ from one another. PSP has orbited and travelled fair amount into the magnetosphere of Venus. Polarity is a powerful tool for characterising the planets of the solar system. Similar to the condition of linear polarisation, the state form of circular polarisation can unlock details about the make-up of a planet's atmosphere as well as its surface characteristics.[7].

The fluctuations in the interaction region between solar wind and Venus have been studied to understand the polarisation of the magnetic field. This examination of magnetic field has been done using software known as amda. All four encounters produced very convincing results. The PSP magnetometer collected magnetic field data at a sampling rate of 1 Hz. For the absolute field, data accuracy is approximately 1 nT, and for the variable field, it is better than 0.1 nT. Utilizing a method for examining the polarisation characteristics of plane waves [1], we studied the properties of waves at very high resolution under the different IMF orientations and time period.

The results from the first encounter is distorted. The polarisation is neither linear nor circular (Fig 16). An unusual disturbed and vague wave structure can be seen. The properties of the waves generated from upstream are fairly mixed and no clear tendency can be found. It might be due to the lost data and technical glitch occurred in the PSP during the encounter. (Fig 16)

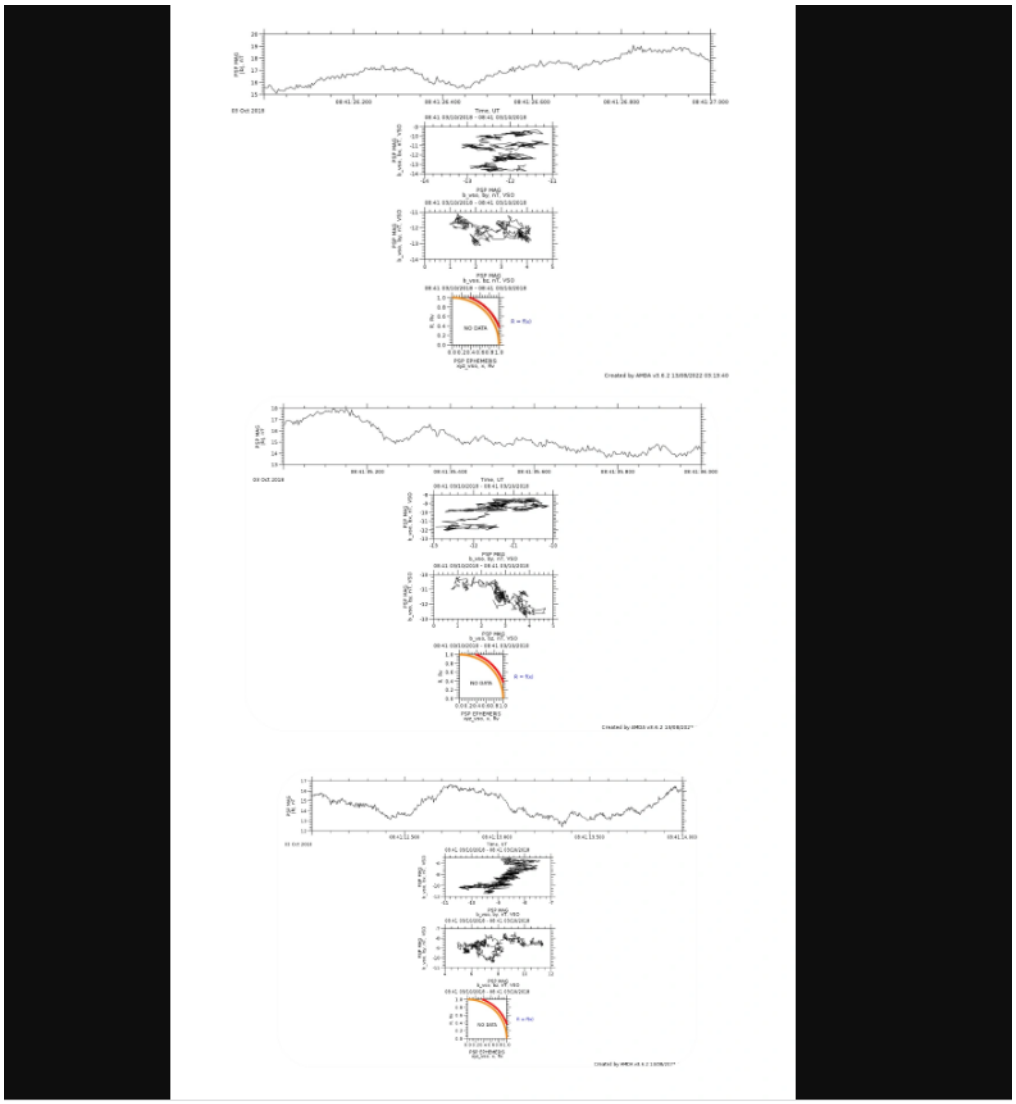

The second encounter produces a circular shaped structure polarisation. From the fig. it can be clearly seen. Through out the whole variations in the magneto-sheath the polarisation is circular (Fig 17).

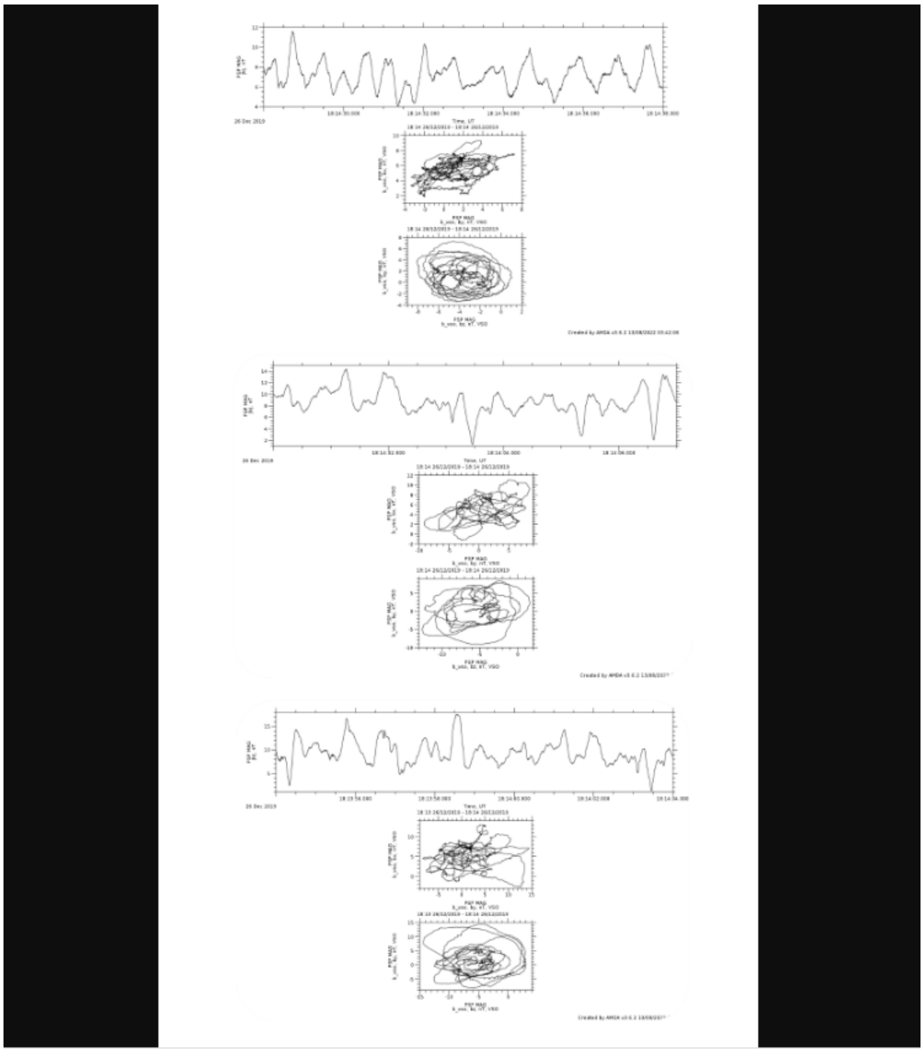

The Venus Flyby 3 and 4 distribution of magnetic field is a combination of both linearly and circular shaped polarisation. Polarisation work has not been done critically. But with more critical analysis of these variations in magnetic field of Venus, and more upcoming data can lead to improvised current understanding of VPE.(Fig 18) and (Fig 19)

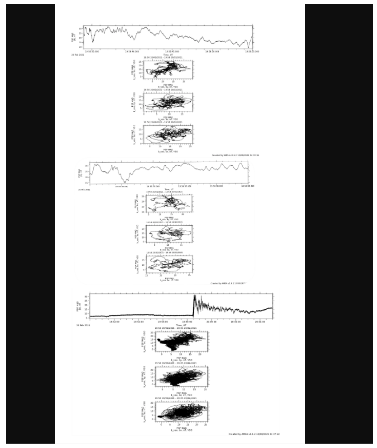

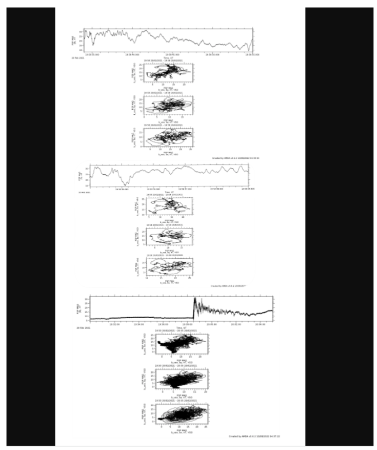

12 Software's

To carry out analysis, two of software are employed: Amda.cddp.edu for data analysis and Python coding language is used for a detailed plotting of position of PSP trajectory and the analysis of magnetic field and its coordinates around Venusian Bow shock.

13 Results

1) It was evident from the data and graphing that every Venus PSP Flyby entered the Venusian BS. PSP travelled to Venus in its closest orbit during encounters 3 and 4. PSP's track during both encounters was quite close to Venus' ionosphere. PSP primarily travelled along the edge of the BS barrier in encounters 1 and 2.

2) With the received data from the encounter 2,3 and 4, we have calculated the position of the BS. The location of BS are shown in Table 1, 2 and 3.

3) For all encounters, information from FIELDs was used to measure the variations in the magnetic field at different time periods. In all four interactions, sharp, rapid, and fast magneto sonic shock waves were seen. A few time intervals between encounters 3 and 4 were noticed, and some fluctuations were not abrupt. In every encounter, the average total magnetic field strength $|b|$ ranged from 5 to 25 nT. The peak measured for overall magnetic strength reached a maximum of 32 nT.

4) Because the distance between the bow shock terminator and the sun's terminator was found to be greater at solar maximum than at solar minimum, PVO measurements have demonstrated that solar activities can affect the shape of the Venusian bow shock [15]. However, the SZA at the Venusian bow shock covered by PVO has a narrow range from 60 to 110 degree [15], making it difficult to pinpoint its precise subsolar location. The Venusian bow shock is covered by the VEX mission over a wider range of SZA (from 10 to 135 degree), and both the standoff and terminator distance of the Venusian bow shock may be precisely measured. [22]. The Venusian bow shock can be shaped by solar activity, according to PSP measurements. However, the range of the SZA at the Venusian bow shock that is covered by PSP current result is from 70 to 110 degrees.

5) In PSP observations, the fluctuations observed in shock around 850 km altitude in the insert of Venus Fly by 3 at solar minimum. It is clear that the effective altitude of the obstacle, derived [7] is very near to 0 km altitude even if the shock is detached, which implies that the obstacle is weak and significant absorption of the solar wind is taking place. In previous missions results, the shock was found to be detached which consistent with out data as well. It was clear from the observation that the shape of bow shock also depend upon on the phases of solar cycle. Although the mach number is low, future research will examine more closely at all values and angles in order to gather more insightful information. The results from earlier experiments can then be compared with the newly discovered values.

6) The crossing geometry of encounter 1 and 2 found to be quasi-perpendicular. While for encounter 3 and 4 it was a combination of both quasi parallel and perpendicular. The angle between position and shock normal for encounter 2, 3 and 4 are in the range of 70 to 110 degree.

7) To comprehend the polarisation of the magnetic field, the variations in the region of the solar wind-Venus interaction have been investigated. The outcomes of the initial meeting are disturbed and vague. The polarisation is not circular or

linear. A polarisation with a circular form is produced by the second encounter. While Flyby 4 solely uses circularly polarised waves, Venus Flyby 3's magnetic field distribution combines both linear and circular polarisation.

14 Discussion and conclusions

Based on the PSP observation, we were able to determine the day side position of the Venusian BS in this research. The observed VEX crossings of the plasma barriers were converted into an aberrated solar ecliptic system by assuming a 5 degree aberration angle. Under the supposition of cylindrical symmetry along the X0 axis, the BS is represented by a conic section expressed in polar coordinates with an offset of the focus that is allowed to wander along the symmetry axis. (i.e., the direction opposite to the solar wind flow direction)[22]. It was discovered that the crossing geometry of encounters 1 and 2 was nearly perpendicular. While it was a combination of quasi parallel and perpendicular for encounters 3 and 4, respectively. The angle between location and shock normal for encounters 2, 3, and 4 was also calculated. Tables 2, 3, and 4 display the angle between location and shock normal for encounters 2, 3, and 4.

Since the size of bow shock is mostly dependent by size of the obstacle, We also looked into the relationship between the terminator BS position and the solar EUV, since the solar wind interaction with Venus depends on the solar cycle's phase. This made it easier to understand how the solar cycle affected the form of the BS. There was no relationship established in the paper but it can be more critically looked in future. Calculating the values of the terminator at various solar wind phases unfortunately becomes too complicated due to the unavailability of all PSP crossings and data sets. However, it is clear from the observation and statistics that the BS position and form around Venus is also influenced by the phases of solar cycles. The variations that Venus Fly by 3's insert recorded at solar minimum at a height of 850 km. At solar minimum the BS is found to be closer to the planet than at solar maximum by PVO, and VEX and we also observed the same behaviour in the PSP encounter 3 . It is evident that the shock's ensemble average location at solar maximum is farther from Venus than it is at solar minimum. However, we may also detect a slight change in the average shock locations between the VEX and PVO data during solar maximum and minimum. [13]. Additionally, we deduce from our findings that the BS location on the night-side is reasonably steady while the ICB position is significantly changeable. The polarisation of magnetic field also been examined. The results were positive and exciting. The fluctuations in the area of the solar wind-Venus interaction have been studied in order to understand the polarisation of the magnetic field. The initial meeting's conclusions are troubling and hazy. There is no circular or linear polarisation. The second encounter results in a polarisation with a circular shape. Venus Flyby 3's magnetic field distribution comprises both linear and circular polarisation, whereas Flyby 4 only employs circularly polarised waves. Further study of this polarisation in future can also reveal many properties about the Venus atmosphere.

15 Future Work

Venus is a crucial body for swing-by operations on the way to the inner (Mercury) and outer (planets) of the solar system (e.g. Jupiter, Saturn). It is therefore envisaged that there will be a number of fly-bys of spacecraft with excellent plasma and field instruments. With more critical analysis of compared results from PVO, VEX and PSP in different solar cycles can improve our understanding. The upcoming PSP Venus flyby's i.e 5, 6 and 7 will be very significant to understand more about VPE. Future careful investigation of bow crossing geometry and varying magnetic field fluctuation along with PVO and VEX data can further clarify our understanding. Other spacecraft have recently identified double-layered plasma in VPE. There is a possibility that we will find further double-layered plasma connections if we carefully analyse the PSP encounter and the data from FIELDs and SWEAP.From PSP data, We can also establish relationship between distant bow shock and sunspot number to understand more about Venus BS comprehensibility. Polarization can be critically analysed to learn more about the Venusian atmosphere.

The field of the solar wind interaction with Venus is directly related to key scientific issues including planetary atmospheric evolution and escape to space, upper atmosphere physics, and ionosphere, etc similar like non-magnetized planets. Precision magnetic field measurements and knowledge of ionospheric currents can be used to distinguish the magnetic field from the induced current in the Venus crust and, lead to, unlock the conductivity of the mantle of Venus, which is correlated with the crust's water content. This is possible because there are no local magnetisation like those on the Moon, Mars and other planets. To understand the evolution of water on Venus, which is a the moment dry, the latter factor is the most important one. Solar Probe Plus,

Solar Orbiter, and JUICE are a few fly-by missions that are crucial for understanding the solar wind. Such flyby missions only provide short-term data, but on the plus side, due to meticulous sensor synchronisation, we have more time to make measurements for the flyby event. In fact, science related to the investigation of the solar wind-Venus interaction will be covered on all subsequent missions.

16 Appendix A

16.1 Plot of PSP encounters with Venus

```
import math
import numpy as np
import matplotlib
from matplotlib import pyplot as plt

circle_theta = np.arange(0,math.pi+0.1,math.pi/90)

circle_x = np.cos(circle_theta)
circle_y = np.sin(circle_theta)

bs_theta = np.arange(0.0,0.77*math.pi,math.pi/90)

L = 1.303
epsilon = 1.056
bs_r = L / (1.0+epsilon*np.cos(bs_theta))
bs_x = 0.788 + bs_r*np.cos(bs_theta)
bs_y = bs_r*np.sin(bs_theta)

fig, ax1 = plt.subplots(nrows=1, ncols=1, figsize=(10,5))

ax1.set_xlabel('x')
ax1.set_ylabel('y')

plt.xlim(-5,2)
plt.ylim(0,5)

ax1.set_aspect('equal')

ax1.plot(circle_x,circle_y)
ax1.plot(bs_x,bs_y)

# VFB 2
x_vso =  -0.661
y_vso = -2.327
z_vso =  -0.118
r = np.sqrt(x_vso*x_vso + y_vso*y_vso + z_vso*z_vso )
theta = math.acos( x_vso/r )
x = r*np.cos(theta)
y = r*np.sin(theta)

ax1.plot(x,y,'X')
```

```
# VFB 2 (BS Second time interval)

x_vso =  -0.259
y_vso =  -2.066
z_vso =  -0.118
r = np.sqrt(x_vso*x_vso + y_vso*y_vso + z_vso*z_vso )
theta = math.acos( x_vso/r )
x = r*np.cos(theta)
y = r*np.sin(theta)

ax1.plot(x,y,'X')

# VFB 2 (BS Third time interval)

x_vso =  0.745
y_vso = -1.303
z_vso =  -0.118
r = np.sqrt(x_vso*x_vso + y_vso*y_vso + z_vso*z_vso )
theta = math.acos( x_vso/r )
x = r*np.cos(theta)
y = r*np.sin(theta)

ax1.plot(x,y,'X')

# VFB 3

x_vso =  0.15
y_vso = -2.2
z_vso =  -1.95
r = np.sqrt(x_vso*x_vso + y_vso*y_vso + z_vso*z_vso )
theta = math.acos( x_vso/r )
x = r*np.cos(theta)
y = r*np.sin(theta)

ax1.plot(x,y,'o')

# VFB 3 (BS Second time interval)

x_vso =  0
y_vso = -1.6
z_vso =  -1.95
r = np.sqrt(x_vso*x_vso + y_vso*y_vso + z_vso*z_vso )
theta = math.acos( x_vso/r )
x = r*np.cos(theta)
y = r*np.sin(theta)
```

```
ax1.plot(x,y,'o')

# VFB 3 (BS Third time interval)

x_vso =  -0.2
y_vso = -1.5
z_vso =  -1.95
r = np.sqrt(x_vso*x_vso + y_vso*y_vso + z_vso*z_vso )
theta = math.acos( x_vso/r )
x = r*np.cos(theta)
y = r*np.sin(theta)

ax1.plot(x,y,'o')

# VFB 4

x_vso =  0
y_vso = -2.5
z_vso =  2.7*10e-3
r = np.sqrt(x_vso*x_vso + y_vso*y_vso + z_vso*z_vso )
theta = math.acos( x_vso/r )
x = r*np.cos(theta)
y = r*np.sin(theta)

ax1.plot(x,y,'v')

# VFB 4 (BS Second time interval)

x_vso =  -0.8
y_vso = -2
z_vso =  2.85*10e-3
r = np.sqrt(x_vso*x_vso + y_vso*y_vso + z_vso*z_vso )
theta = math.acos( x_vso/r )
x = r*np.cos(theta)
y = r*np.sin(theta)

ax1.plot(x,y,'v')

ax1.plot(0.5,2.2,'*','o','v')

plt.show()
```

16.2 Magnetic field fluctuations with its coordinates

```
import numpy as np
```

```
import matplotlib
from matplotlib import pyplot as plt
import numpy as np
import datetime as dt
import cdflib

# define the folder name for the data files, and the data file names
data_folder = 'gdrive/MyDrive/PSP_VFB2_data/PSP_VFB2_data/'
ephem_file = 'spp_fld_l1_ephem_spp_vso_20191228_v00.cdf'
#psp_mag_VSO_fname1 = 'psp_fld_l2_mag_VSO_2019122612_v01.cdf';
psp_mag_VSO_fname2 = 'psp_fld_l2_mag_VSO_2019122618_v01.cdf';
#psp_mag_VSO_fname3 = 'psp_fld_l2_mag_VSO_2019122618_v01.cdf';


# open the CDF ephemeris file
ephem_cdf_file = cdflib.CDF(data_folder+ephem_file)
#ephem_cdf_file = cdflib.CDF(data_folder+psp_mag_VSO_fname3)
#print("type is :", type(ephem_cdf_file))
cdf_file_info = ephem_cdf_file.cdf_info()
print("info = ",cdf_file_info)
print(type(cdf_file_info))
print( "variables ="  , cdf_file_info["zVariables"])


# get all the data in the file for the named variables
# the data is the time tags, and then spacecraft position

print("type = ",type(ephem_cdf_file))
#NameOfVar = None
psp_vfb2_ephem_epoch_ttags = ephem_cdf_file.varget("epoch")

# convert the timetags to datetime as used by numpy
psp_vfb2_ephem_dt_ttags = cdflib.cdfepoch.to_datetime(psp_vfb2_ephem_epoch_ttags, to_np=True


print('Data type of epoch time tags array: ',type(psp_vfb2_ephem_epoch_ttags))
print('Data type of each epoch time tag: ',type(psp_vfb2_ephem_epoch_ttags[10]))
print('Data type of datetime time tags array: ',type(psp_vfb2_ephem_dt_ttags))
print('Data type of each datetime time tag: ',type(psp_vfb2_ephem_dt_ttags[10]))

psp_vfb2_VSO_position = ephem_cdf_file.varget('position')
psp_vfb2_VSO_velocity = ephem_cdf_file.varget('velocity')

print('Data type VSO_position:',type(psp_vfb2_VSO_position))

# calculate positionin VSO in Rv (ie venus radius) - conversion from km
```

```
psp_vfb2_VSO_position_Rv = (1.0/6051.8)*psp_vfb2_VSO_position

# calculate range from Venus
# use linalg.norm to compute magnitude of vector
# note use of axis, so that we get back an array of distances to Venus

psp_vfb2_venus_range_Rv = np.linalg.norm(psp_vfb2_VSO_position_Rv,axis=1)


ephem_cdf_file.close()

# this ends reading the ephem file

# set time range for plots

timerange = [dt.datetime(2019, 12, 26,18,00,0),dt.datetime(2019, 12, 26,18,30,0) ]

# arrange panels, and share the x (ie time) axis so all panels have same time range

# axes will be an array of axes to be used for plotting different quantities

fig, axes = plt.subplots(nrows=3, ncols=1,sharex=True)
fig.tight_layout()


# limit to a given time range by using logical indexing for arrays
#ephem_ttag_mask = (psp_vfb2_ephem_ttags > timerange[0]) & (psp_vfb2_ephem_ttags <= timerang

#plt.plot(psp_vfb2_ephem_ttags[ttag_mask],psp_vfb2_venus_range_Rv[ttag_mask])

#alternative
# Zoom in by setting axis limits
axes[0].plot(psp_vfb2_ephem_dt_ttags,psp_vfb2_venus_range_Rv)

axes[0].set_ylim(0.0, 12.0)
axes[0].set_xlim(timerange[0],timerange[1])
#axes[0].set_title('PSP VFB2')
axes[0].set_ylabel('Venus range ($R_V$)')



# Next - read in the magnetic field data


psp_mag_122618_cdf = cdflib.CDF(data_folder+psp_mag_VSO_fname2)
```

```
print(psp_mag_122618_cdf)

psp_vfb2_mag_epoch_ttags = psp_mag_122618_cdf.varget("epoch_mag_VSO")

# convert the timetags to datetime as used by numpy
psp_vfb2_mag_ttags = cdflib.cdfepoch.to_datetime(psp_vfb2_mag_epoch_ttags, to_np=True)


psp_vfb2_mag_VSO = psp_mag_122618_cdf.varget("psp_fld_l2_mag_VSO")

print('size/shape of mag data: ',psp_vfb2_mag_VSO.shape )

# construct a logical mask for timetags in time range

mag_ttag_mask = (psp_vfb2_mag_ttags > timerange[0]) & (psp_vfb2_mag_ttags <= timerange[1])

print('done mask')

# extract just the elements for the time range being plotted
# this makes plotting much faster!

mag_ttags = psp_vfb2_mag_ttags[mag_ttag_mask]
magVSO_Bx = psp_vfb2_mag_VSO[mag_ttag_mask,0] # Bx component
magVSO_By = psp_vfb2_mag_VSO[mag_ttag_mask,1] # By
magVSO_Bz = psp_vfb2_mag_VSO[mag_ttag_mask,2] # Bz

magVSO_Btot = np.linalg.norm(psp_vfb2_mag_VSO[mag_ttag_mask,:],axis=1)

print(magVSO_Btot.shape)

axes[1].plot(mag_ttags, magVSO_Btot )
axes[2].plot(mag_ttags, magVSO_Bx )
axes[2].plot(mag_ttags, magVSO_By )
axes[2].plot(mag_ttags, magVSO_Bz )

axes[1].set_ylabel('B total (nT)')
axes[2].set_ylabel('B xyz (nT)')

plt.show()
```

References

[1] CW Arthur, RL McPherron, and JD Means. A comparative study of three techniques for using the spectral matrix in wave analysis. *Radio Science*,

11(10):833–845, 1976.

[2] Stephen H Brecht and John R Ferrante. Global hybrid simulation of unmagnetized planets: Comparison of venus and mars. *Journal of Geophysical Research: Space Physics*, 96(A7):11209–11220, 1991.

[3] Zoltan Dobe, Andrew F Nagy, Larry H Brace, Thomas E Cravens, and Janet G Luhmann. Energetics of the dayside ionosphere of venus. *Geophysical research letters*, 20(15):1523–1526, 1993.

[4] Sh Sh Dolginov, EG Yeroshenko, and LN Zhuzgov. Magnetic field investigations with ais"venera-4". Technical report, NASA. GODDARD SPACE FLIGHT CENTER, 1968.

[5] Mostafa El-Alaoui, Robert L Richard, Maha Ashour-Abdalla, and Margaret W Chen. Low mach number bow shock locations during a magnetic cloud event: Observations and magnetohydrodynamic simulations. *Geophysical research letters*, 31(3), 2004.

[6] Yoshifumi Futaana, Gabriella Stenberg Wieser, Stas Barabash, and Janet G Luhmann. Solar wind interaction and impact on the venus atmosphere. *Space Science Reviews*, 212(3):1453–1509, 2017.

[7] James E Hansen and JoW Hovenier. Interpretation of the polarization of venus. *Journal of Atmospheric Sciences*, 31(4):1137–1160, 1974.

[8] Takuya Hara, Zesen Huang, David L Mitchell, Gina A DiBraccio, David A Brain, Yuki Harada, and Janet G Luhmann. A comparative study of magnetic flux ropes in the nightside induced magnetosphere of mars and venus. *Journal of Geophysical Research: Space Physics*, 127(1):e2021JA029867, 2022.

[9] AM Krymskii, TK Breus, NF Ness, and MH Acuña. The imf pile-up regions near the earth and venus: lessons for the solar wind-mars interaction. *Space Science Reviews*, 92(3):535–564, 2000.

[10] Janet G Luhmann and SJ Bauer. Solar wind effects on atmosphere evolution at venus and mars. *Washington DC American Geophysical Union Geophysical Monograph Series*, 66:417–430, 1992.

[11] C Martinecz, M Fränz, J Woch, N Krupp, E Roussos, E Dubinin, U Motschmann, S Barabash, R Lundin, M Holmström, et al. Location of the bow shock and ion composition boundaries at venus—initial determinations from venus express aspera-4. *Planetary and Space Science*, 56(6):780–784, 2008.

[12] KR Moore, DJ McComas, CT Russell, SS Stahara, and JR Spreiter. Gasdynamic modeling of the venus magnetotail. *Journal of Geophysical Research: Space Physics*, 96(A4):5667–5681, 1991.

[13] CT Russell, E Chou, JG Luhmann, P Gazis, LH Brace, and WR Hoegy. Solar and interplanetary control of the location of the venus bow shock. *Journal of Geophysical Research: Space Physics*, 93(A6):5461–5469, 1988.

[14] RE Shefer, AJ Lazarus, and HS Bridge. A reexamination of plasma measurements from the mariner 5 venus encounter. *Journal of Geophysical Research: Space Physics*, 84(A5):2109–2114, 1979.

[15] JA Slavin, RC Elphic, and CT Russell. A comparison of pioneer venus and venera bow shock observations: Evidence for a solar cycle variation. *Geophysical Research Letters*, 6(11):905–908, 1979.

[16] JA Slavin, EJ Smith, JR Spreiter, and SS Stahara. Solar wind flow about the outer planets: Gas dynamic modeling of the jupiter and saturn bow shocks. *Journal of Geophysical Research: Space Physics*, 90(A7):6275–6286, 1985.

[17] OL Vaisberg, SA Romanov, VN Smirnov, IP Karpinsky, BI Khazanov, BV Polenov, AV Bogdanov, and NM Antonov. Ion flux parameters in the solar wind-venus interaction region according to venera-9 and venera-10 data. *Physics of Solar Planetary Environments*, 2:904–917, 1976.

[18] SD Xiao, TL Zhang, and Z Vörös. Magnetic fluctuations and turbulence in the venusian magnetosheath downstream of different types of bow shock. *Journal of Geophysical Research: Space Physics*, 123(10):8219–8226, 2018.

[19] SD Xiao, TL Zhang, Zoltán Vörös, MY Wu, GQ Wang, and YQ Chen. Turbulence near the venusian bow shock: Venus express observations. *Journal of Geophysical Research: Space Physics*, 125(2):e2019JA027190, 2020.

[20] Q Xu, X Xu, TL Zhang, ZJ Rong, M Wang, J Wang, Y Ye, Z Zhou, Q Chang, J Xu, et al. The venus express observation of venus' induced magnetosphere boundary at solar maximum. *Astronomy & Astrophysics*, 652:A113, 2021.

[21] MHG Zhang, JG Luhmann, and AJ Kliore. An observational study of the nightside ionospheres of mars and venus with radio occultation methods. *Journal of Geophysical Research: Space Physics*, 95(A10):17095–17102, 1990.

[22] TL Zhang, W Baumjohann, M Delva, H-U Auster, A Balogh, CT Russell, S Barabash, M Balikhin, G Berghofer, HK Biernat, et al. Magnetic field investigation of the venus plasma environment: Expected new results from venus express. *Planetary and Space Science*, 54(13-14):1336–1343, 2006.

[23] TL Zhang, KK Khurana, CT Russell, MG Kivelson, R Nakamura, and W Baumjohann. On the venus bow shock compressibility. *Advances in Space Research*, 33(11):1920–1923, 2004.

[24] TL Zhang, JG Luhmann, and CT Russell. The magnetic barrier at venus. *Journal of Geophysical Research: Space Physics*, 96(A7):11145–11153, 1991.